



Observation of mesenteric microcirculatory disturbance in rat by laser oblique scanning optical microscopy

Yichen Ding^{1*}, Yu Zhang^{2*}, Tong Peng¹, Yiqing Lu⁴, Dayong Jin⁴, Qiushi Ren¹, Yuying Liu², Jingyan Han^{2,3} & Peng Xi¹

¹Department of Biomedical Engineering, College of Engineering, Peking University, No. 5 Yiheyuan Road, Beijing 100871, China, ²Department of Integration of Chinese and Western Medicine, School of Basic Medical Science, Peking University, 38 Xueyuan Road, Beijing 100191, China, ³Tasly Microcirculation Research Center, Peking University Health Science Center, Beijing 100191, China, ⁴Advanced Cytometry Labs, MQphotonics Research Centre, Macquarie University, NSW 2109, Sydney, Australia.

Ischemia-reperfusion (I/R) injury model has been widely applied to the study of microcirculation disturbance. In this work, we used laser oblique scanning optical microscopy (LOSOM) to observe the microcirculation system in the mesentery of rat model. Utilizing a localized point-scanning detection scheme, high-contrast images of leukocytes were obtained. The extended detection capability facilitated both the automatic *in vivo* cell counting and the accurate measurement of the rolling velocity of leukocytes. Statistical analysis of the different treatment groups suggested that the distinction between I/R and sham groups with time lapse is significant.

The application of optical microscopy in biological observation is very straightforward, but often challenging as biological specimens are usually lack of sufficient contrast. To increase the contrast, staining (both with chromatic and fluorescent dyes) has been widely employed, especially in the field of cellular and tissue sectional imaging¹. However, because the staining may alter the biological process of interest, and that the result of imaging can also be affected by staining efficiency and its different protocols, the staining-based approaches can not be applied to many clinical applications². One solution to improving weak (low contrast) signal detection, is to increase the sensitivity of the detector, for example, by using multiplying amplified detectors such as photo-multiplier tubes (PMT) or by using an electron multiplying charge coupled device (EMCCD). For instance, benefiting from its high sensitivity of the point detecting PMT, the confocal laser scanning microscopy (CLSM) has been widely used in both biological cellular study³ and clinical imaging⁴. We have reported that, with the reflection and autofluorescence of the biological tissue, early diagnosis of melanoma is possible with multi-modality confocal microscopy⁵. Yet, as normal tissues have relatively low concentration of high-refractive index components such as melanin, these can be difficult to visualize directly with adequate signal-to-background contrast ratio.

To overcome the difficulty of the weak signal detection, we have previously developed a new image contrast mechanism, which we termed Laser Oblique Scanning Optical Microscopy (LOSOM), in which a fluorescent contrast enhancing medium is employed above the specimen, to serve as a new oblique light source for illumination of the specimen⁶. Taking advantage of its localized illumination feature and the sensitivity of the single point detector such as a PMT, LOSOM has demonstrated greater sensitivity than that shown with conventional microscopy. We have shown that, even with highly fluorescent stained specimen, LOSOM can overcome this unwanted signal and still provide phase-relief imaging.

In this study, we applied LOSOM to the visualization of dynamic pathophysiological changes *in vivo*, and we demonstrated the capability of enhancing the local contrast of the absorption imaging. We chose a rat mesentery ischemia-reperfusion (I/R) injury model to observe the microcirculation disorders intravitaly. I/R injury occurs in a wide range of pathological changes and diseases, including trauma, vascular reflow after contraction, percutaneous transluminal coronary angioplasty, thrombolysis treatment, organ transplantation, and hypovolemic shock with resuscitation⁷, leading to systemic disorders and high morbidity and mortality outcomes. I/R

SUBJECT AREAS:

MICROSCOPY

BIOLOGICAL TECHNIQUES

BIOMEDICAL ENGINEERING

OPTICAL IMAGING

Received

25 January 2013

Accepted

15 April 2013

Published

3 May 2013

Correspondence and requests for materials should be addressed to J.Y.H. (hanjingyan@bjmu.edu.cn) or P.X. (xipeng@pku.edu.cn)

* These authors contributed equally to this work.

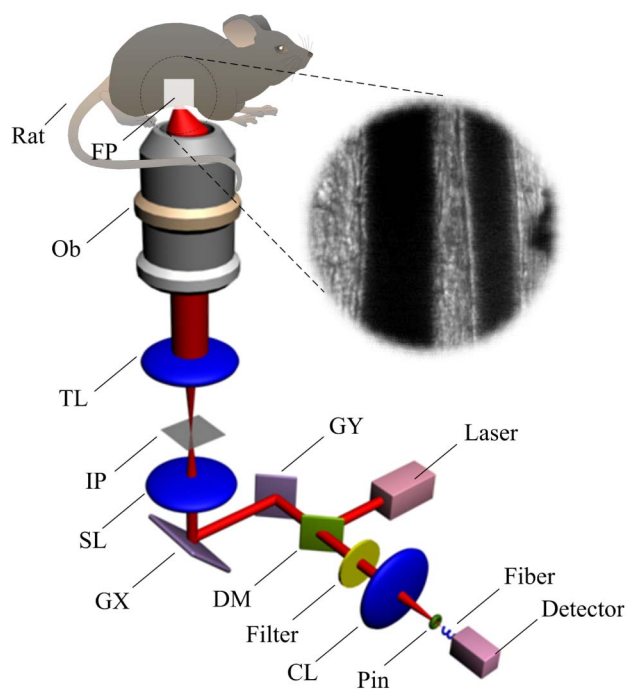


Figure 1 | Schematic LOSOM system for *in vivo* rat mesenteric microcirculatory monitoring. FP: fluorescent plate; Ob: objective (NA = 0.3, Nikon, Japan); TL: tube lens; IP: intermediate plane; SL: scan lens; GX: galvanometer-x; GY: galvanometer-y; DM: dichroic mirror; CL: collecting lens; Pin: pinhole.

induced microcirculatory disturbance is the pathological basis of I/R injury, which consists of injury of endothelial cells, adhesion of leukocytes^{8,9}, production of oxygen radicals^{10–12}, and degranulation of mast cells^{12,13}. Rat mesentery I/R model is a commonly used I/R model for the study of microcirculatory dysfunction^{11,14–17}. In this report we used the LOSOM system to observe leukocytes rolling and adherent in rat mesentery (see schematic Figure 1). High contrast images of the rolling leukocytes can be obtained with our LOSOM technique as it facilitates automatic cell counting with extended capability for accurate velocity analysis. In this study, statistical analysis of the data suggests that the distinction between I/R and sham groups after time lapse is significant ($p < 0.05$). The successful demonstration of LOSOM with this I/R model suggests a novel analytical approach to the study of microcirculation pathology.

Results

Figure 1 illustrates the setup of the LOSOM system for *in vivo* monitoring of the rat mesenteric microcirculation. Details of the system can be found in Methods and Materials. Figure 2 shows different locations of the mesentery tissue of the rat. LOSOM is able to clearly

differentiate the adipose tissue, blood vessels and lymphatic vessels. By adjusting the focal plane and illumination angle⁶, the appearance of the tissue differs and is presented as Figure 2a, 2b and 2c. The surrounding tissue appears in pseudo-three dimension due to the phase-relief imaging capability of LOSOM (Figure 2c), which offers additional information of optical thickness during the same scanning procedure (Figure 2a and 2b). In the following study, we study the leukocytes rolling and adhesion in venules instead of arteries or arterioles, because the speed of blood flow in venules is gradual enough to be observed with LOSOM.

Figure 3 consists of eight successive frames and an image (Figure 3a) as a baseline at the beginning of observation. Most leukocytes flowed with the erythrocytes, and are difficult to distinguish and capture. However, when endothelial cells are dysfunctional, some leukocytes slow down and roll along the venular wall, or become adherent to the vessels where they usually produce reactive oxygen species. In Figure 3a, the yellow arrows indicate the venule and the capillary respectively. Leukocytes were seldom visualized during observation. After 90 minutes in the frames Figure 3(b–j), some leukocytes marked by red arrows, were adherent to the venular wall. In these images, due to different places shown in the registered images, rolling leukocytes indicated by the blue arrows were also detected.

By measurements of the distance traveled by one leukocyte between two frames, its moving velocity was calculated. As shown in Figure 4, four images were acquired over a four second sequence, and demonstrate a leukocyte (indicated by a white arrow) in each frame rolling along the venular wall. After measuring the vertical distance and angle between the vessel and horizontal direction, the speed of its shifting was nearly $38.5 \pm 7.2 \mu\text{m/s}$. Notably, if the direction of vessel is parallel to the scanning direction, the leukocyte may be extended to a short line in a single frame due to the relatively slow imaging speed (1fps). The rate could also be analyzed from the relationship between scanning speed and quantity of occupied pixels if the size of leukocyte can be assumed to a specified shape.

Twelve rats were divided into two groups: one was induced by I/R, while the other was manipulated as a sham group. Figure 5a is an average of ten images, corresponding to single frame 5b at the same time. 5c is a subtraction result between 5a and 5b, that is, 5a is treated as a baseline or background of 5b. Thus, the Figure 5c is acquired as “ $c = b - a$ ”. Based on the analysis procedure described in the section on Data processing in the Materials and Methods section, the number of leukocytes in 5c is counted to be twelve, and is shown in 5d labeled with its corresponding numbers. In Figure 5d, some areas are shown with suspect white points without numbers labeled and are probably the leukocytes situated beyond the focal plane since their sizes mismatch the desired size of a leukocyte. The image processing is thus confined to the analysis of the quantity of leukocytes within the focal zone. The red arrows among 5b to 5d are all indicating the same cells. By filtering out the background signal, cell counting can become automatic, and incur less interference from artificial errors

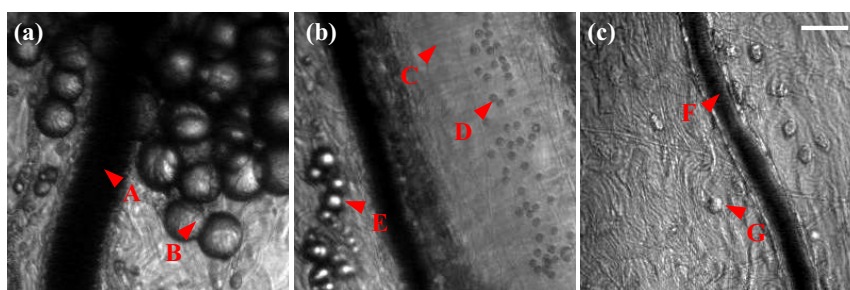


Figure 2 | Different locations of a rat mesentery under the LOSOM. (a) A is the root of a venule and B denotes ambient adipose tissue. (b) C indicates a lymphatic vessel; D points lymphocytes and E marks adipose tissue. (c) F is a mesenteric arteriole and G shows surrounding mast cells. Scale bar: 30 μm .

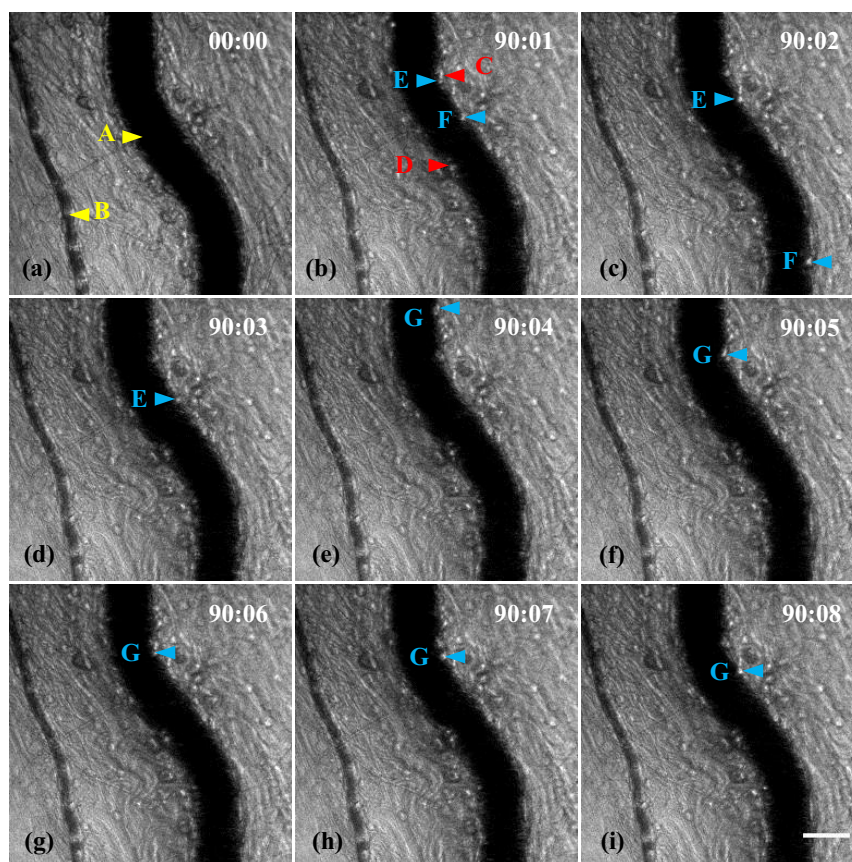


Figure 3 | Time lapse results of adherent and rolling leukocytes in a rat mesenteric venule *in vivo*. (a) is the beginning of an observation, as a baseline, and the yellow arrow A denotes a mesenteric venule while the yellow arrow B is a capillary. (b)–(i) Series of observation of leukocytes rolling after 90 minutes has elapsed. Compared to (a), C, D cells indicated by red arrows are adherent leukocytes, and the other cells (E, F and G) indicated by blue arrows are rolling leukocytes along the venular wall. From (b) to (i), the time interval is 1 second. Scale bar: 30 μm .

resulting in a higher analytical speed. Following such an analytical procedure, the numbers of counted cells from each of these twelve rats for the same observation duration (0 to 90 min) are presented as Figure S1 in the Supplementary Information document.

Figure 6(a–e) shows a time-lapse series of processed images of leukocytes in a typical sample from the I/R group for 90 min (see Movie S1 and S2), while Figure 6(f–j) are sampled from the sham group (see Movie S3 and S4). In order to present surrounding background of each sample, 6a and 6f are treated as the original average images. Figure 6k is the statistical result for the I/R group, when normalizing all data to baseline. After statistically analyzing using the one-way ANOVA with Turkey post-test calculation at different time points, Figure 6k reveals the relationship between the number of leukocytes and the time taken. Although it fluctuates largely (see the minimum to maximum numbers at each time point), the accumulation of leukocytes increases with time lapse after the I/R is induced.

Compared to the baseline, the differences in number of leukocytes are significant ($p < 0.05$) at 60 min, and extremely significant ($p < 0.001$) at 90 min. Similarly, it is highly significant ($p < 0.01$) when the result is compared for the 90 min and 10 min segment. Figure 6l compares I/R and sham groups at different time, when normalizing all data to its own baseline. Two-way ANOVA with Bonferroni post-test method is employed to reveal the interaction between two factors, time and treated methods. From the present result in 6l, it is clear that no matter what operated method, I/R or sham, the quantity of the leukocytes increases with the time taken. However, the growth ratio coming from different groups is distinct. At 90 min, the growth ratio of quantity of accumulated leukocyte in I/R group has a significant difference ($p < 0.05$) compared with that of the sham group. Therefore, our experiment reveals how these two factors, the time taken and the treatment methods, influence the growth ratio of leukocytes in mesenteric venules of a rat model.

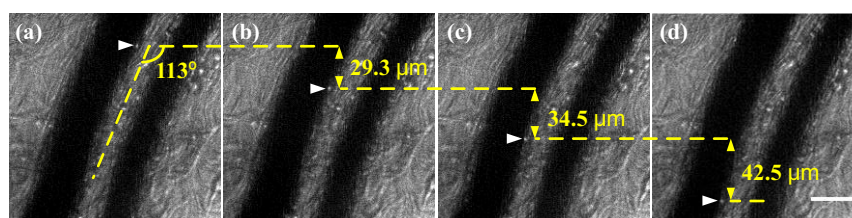


Figure 4 | Tracking one rolling leukocyte along the venular wall to simply estimate the rate of leukocyte rolling in a rat mesenteric venule. Compared to a former panel, the relative vertical distance is 29.3 μm (b–a), 34.5 μm (c–b) and 42.5 μm (d–c), respectively. The average angle between vessels and horizontal direction is 113° . Time interval of sequent image is 1 second. Scale bar: 30 μm .

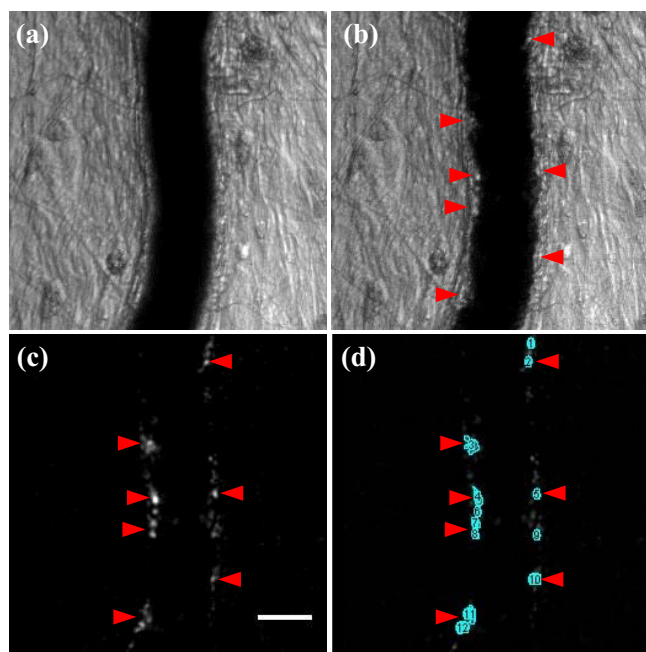


Figure 5 | Results of cell counting. (a) The average of 10 sequent venular images at the beginning of observation, act as a baseline. (b) Single frame of instantaneous blood flow containing leukocytes (red arrows), corresponding to the same experimental conditions as the baseline. (c) Processed Result of (b–a), arrows correspond to (b), scale bar: 30 μm . (d) Result of cell counting analyzed with ImageJ, with cells labeled by numbers.

Discussion

Since there are anastomotic branches between the mesentery artery and the vein, merely clipping the superior mesenteric artery (SMA) would not completely occlude the blood flow. In addition, SMA clipping with high pressure damages the vessel wall, while at low pressure would not block the blood flow effectively. Therefore, we tested an improved approach to establishing the mesentery ischemia and reperfusion model, i.e., occluding the mesentery artery and the corresponding vein simultaneously. Our previous research demonstrated that ligating the feeding branch of the anterior mesenteric artery and the corresponding vein simultaneously, consistently ensures the establishment of an ischemia model^{14,15}. It's worthy of note that the simultaneous ligation of the SMA and the superior mesenteric vein is one of the classic mesentery ischemia and reperfusion models, and is as commonly used as SMA clapping^{14,15,18,19}. In this experiment, our focus was the observation of leukocytes rolling and adhesion. The blood flow in arteries or arterioles is too fast to observe the leukocytes rolling and adhesion after reperfusion. Therefore, venules have been commonly used to study the leukocytes rolling and adhesion^{20–26}.

LOSOM is applicable to organs with high transparency (low scattering) and tissues that are accessible, such as the mouse ear, interdigital skin, intestine, the edge of hepatic lobe, the subcutaneous tissue, or the cremaster muscle, etc. Other specimen such as cells, zebra fish, embryos etc. are also compatible with this technique, owing to their overt transparency. The imaging depth is limited by the scattering nature of the tissue, just as in other optical microscopy techniques. We have tested the phototoxicity of excitation light at 375 nm using human umbilical vein endothelial cells. The result showed that the cell death rate remained at 9% after 30 seconds of illumination (original condition) and was not significantly different to the control group which was at 6%. However, the cell death rate increased to 25% after 300 seconds of illumination, demonstrating that excitation light at 375 nm is safe when used with our original experimental condition, but will become phototoxic if the dose

increases by 10 fold. Details of this can be seen in Figure S2 in the Supplementary Information document. As the contrast in LOSOM is provided by the difference of absorption or refractive index, longer wavelengths can be used with its corresponding fluorescent medium. The advantage of using longer wavelength is that not only does it provide better contrast due to less scattering, but it can also be less phototoxic to the specimen observed.

In conclusion, we demonstrated the application of LOSOM to the monitoring of the mesentery microcirculation *in vivo* in rats, especially to the imaging and counting of rolling and adherent leukocytes in an I/R injury rat model with a sham control. LOSOM offers a new platform for the high-contrast staining-free imaging of the condition and velocity of cells such as leukocytes, but also with cells such as lymphocytes, mast cells and adipocytes. After the subtraction of the static background, this technique also offers the extended capability for the automation of cell counting. Hence, it provides greater accuracy and faster processing speed with minimized errors, compared to that found with manual microscopic counting. Taking advantage of its point-scanning detection sensitivity, LOSOM has achieved higher signal-to-background ratio than its wide-field counterparts. Thus, the high-contrast label-free imaging of biological tissues, as shown in this study, is now more practical.

Future work on LOSOM could explore its performance in multi-modality imaging applications for enhancing the observation of the microcirculation. Primarily, LOSOM could be used for more rapid scanning and image acquisition, and may benefit broader applications of real-time *in vivo* imaging of many dynamic process in biological samples^{27–29}. The imaging speed is limited by two factors: (1) the sensitivity of the PMT detector and the fluorescent light generated by the fluorescent medium. As the imaging contrast is based on the absorption difference between the leukocytes and the surrounding erythrocytes, this can be readily accelerated when strong fluorescent medium is employed, or with a high speed detector that has a low noise level. (2) The speed of galvanometric scan can be improved by scanning a smaller field of view (FOV) or rectangular FOV with a higher aspect ratio, or by using alternative scanning mechanism, such as a resonant scan or polygon mirror scan. Moreover, because LOSOM has its inherent capability to image fluorescent samples⁶, it becomes feasible to study the reactive oxygen species generated by the leukocyte movement after I/R injury in the mesentery of rat, based on the applications of responsive molecular probes. It may be further likely that it could provide a manifest direction for the drug delivery against I/R induced microcirculatory disturbance.

Methods

Animals. Male Wistar rats weighing 200–250 g were obtained from the Animal Center of Peking University Health Science Center (SCXK 2006–0008). The animals were housed in an environment with temperature of $24 \pm 1^\circ\text{C}$, relative humidity of $50 \pm 1\%$ and a light/dark cycle of 12/12 hr. They were given tap water and standard laboratory rodent chow (Animal Center of All Animals Peking University Health Science Center).

Previous to the experiment, rats were fasted for 12 hr but allowed to freely drink. All animals were handled according to the ethical guidelines of the Peking University Animal Research Committee, and the surgical procedures and experimental protocol were approved by the Committee on the Ethics of Animal Experiments of the Health Science Center of Peking University (LA2011–38).

Microcirculation observation and I/R operation. The rats were anesthetized with urethane (2 g/kg body weight, i.m.), and the right jugular vein was cannulated for saline infusion. After abdomen opened (2–3 cm long middle incision), an ileocecal portion of the mesentery was gently mounted on a transparent plastic stage designed for the rat. The mesentery was kept warm and moist by continuous superfusion with normal saline at 37°C . The whole rat was placed on a stage of an inverted microscope (TE2000E, Nikon, Japan), but illuminated and detected by LOSOM instead of wide-field microscope. Single unbranched venule with diameter ranging between 30 and 50 μm and length longer than 200 μm was selected for the study¹⁵.

After 10 min of basal observation of the rat mesenteric microcirculation, the I/R was accomplished by ligating the feeding branch of the anterior mesenteric artery and the corresponding vein simultaneously with a snare created from polyethylene tube for 10 min and subsequent release of the blood flow. Erythrocyte velocity in the vessels during the ischemia was not zero because of the possible collateral perfusion to

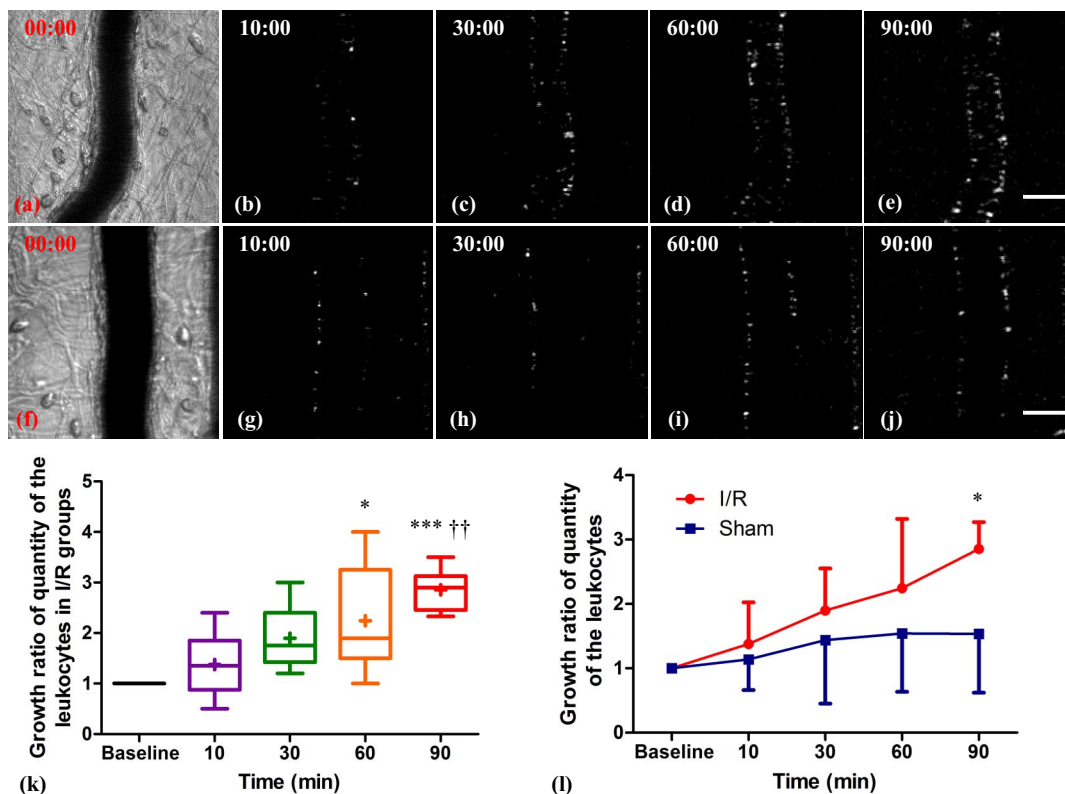


Figure 6 | Comparison of quantity of leukocytes in the mesenteric venules of rats between I/R induced injury (a–e) and sham (f–j) groups. (a) and (f) are original data, treated as baselines. (b–e) and (g–j) are changes in the number of leukocytes at different time points 10 min, 30 min, 60 min and 90 min, respectively. Scale bar: 30 μ m. (k) Result of one-way ANOVA with Turkey post-test analysis, showed a significant result with the time course of the changes in the number of leukocytes in the I/R group. * $p < 0.05$ vs baseline; *** $p < 0.001$ vs baseline; † $p < 0.01$ vs 10 min. The whiskers show the minimum and maximum at different time, respectively. The short lines in box are median values of different groups at different time. The plus “+” indicate the mean values at different time. (l) Result of two-way ANOVA with Bonferroni post-test analysis, shows an interaction between two factors, manipulated methods and time for two groups, I/R and sham groups. * $p < 0.05$ vs sham group.

the observed area. Thus both artery and vein were ligated to stop blood supply and induce venule congestion to enhance ischemia. A previous study showed that 10-min ischemia followed by reperfusion was long enough to induce mesenteric microcirculatory disturbance with minimum intestinal tissue injury³⁰. Sham-operated rats without ligation were used as control¹⁵.

LOSOM instrumentation. LOSOM setup and theorem analysis have been described in^{5,6} at great detail. For details of the resolutions and exposure time of this study can be found in Supplementary Information document. In Figure 1, the anesthetic rat was plated on an object stage, while covering a piece of printing paper (2 cm \times 2 cm in size, as a fluorescent medium) above the observed mesentery outside the body. Because of the paper does not contact the mesentery, potentially external influence on the microcirculation is unlikely. First, the 375 nm laser scans a raster plane after passing through two galvanometers (Nutfield Technology, USA), and then excites the fluorescent medium above the mesentery tissue to emit fluorescence, in order to illuminate the observation area of interest. Next, a dichroic mirror and a bandpass filter were used to separate the wavelength with mesenteric information of the light path so that there was no mixing of laser and fluorescence illumination. Finally, the fiber-based PMT (H9305-02, Hamamatsu, Japan) collected the fluorescent signals transmitting through the dichroic mirror to the image frame (shown in the zoom-in panel in Figure 1).

Data processing. Single frame images of Figure 2–6 are presented in raw data. Averaged images of Figure 5–6 were calculated from 10 sequent frames registered with Rigid Body Registration by the plugin of StackReg in ImageJ³¹. The processed images in Figure 5 and 6 are acquired by subtraction, that is, single frame subtracts corresponding to the average image. In this work, the field of view is set to 200 \times 267 μ m, with 300 \times 400 pixels per image. The pixel dwell time is 8.3 μ s, with the frame rate at 1fps. The lateral and axial resolution are measured to be 1.23 μ m and 13.15 μ m, respectively (see Figure S3 in Supplementary Information). Based on prior knowledge, the size of each leukocyte is estimated around 6–10 μ m, so the processed images the diameter is equivalent to 9–15 pixels.

Statistical analysis. Data was reported as Mean \pm SD, with SD the abbreviation for standard deviation. Statistical analyses are performed using statistical analysis software (GraphPad Prism, version 5.0). ANOVA is the abbreviation for Analysis of

Variance. P values of less than 0.05, 0.01, 0.001 are considered statistically significant, highly significant, and extremely significant, respectively.

- Cox, G. *Optical Imaging Techniques in Cell Biology*. (CRC Press, 2012).
- Freudiger, C. W. *et al.* Label-free biomedical imaging with high sensitivity by stimulated Raman scattering microscopy. *Science* **322**, 1857–1861 (2008).
- Pawley, J. *Handbook of Biological Confocal Microscopy*. (Springer, 2006).
- Petroll, W. M., Cavanagh, H. D. & Jester, J. V. Clinical confocal microscopy. *Curr. Opin. Ophthalmol.* **9**, 59–65 (1998).
- Peng, T. *et al.* CRAFT: Multimodality confocal skin imaging for early cancer diagnosis. *J. Biophotonics* **5**, 469–476 (2012).
- Ding, Y. *et al.* Laser oblique scanning optical microscopy (LOSOM) for phase relief imaging. *Opt. Express* **20**, 14100–14108 (2012).
- Han, J. Y. *et al.* Ameliorating effects of compounds derived from *Salvia miltiorrhiza* root extract on microcirculatory disturbance and target organ injury by ischemia and reperfusion. *Pharmacol. Therapeut.* **117**, 280–295 (2008).
- Granger, D. N. Role of xanthine oxidase and granulocytes in ischemia-reperfusion injury. *Am. J. Physiol. -Heart C.* **255**, H1269–H1275 (1988).
- Guo, J. *et al.* Protective effects of dihydroxyphenyl lactic acid and salvianolic acid B on LPS-induced mesenteric microcirculatory disturbance in rats. *Shock* **29**, 205–211 (2008).
- Han, J. Y. *et al.* Compound Danshen injection improves endotoxin-induced microcirculatory disturbance in rat mesentery. *World J. Gastroenterol.* **13**, 3581–3591 (2007).
- Horie, Y. *et al.* Herbal cardioprotective pills prevent gut ischemia/reperfusion-induced hepatic microvascular dysfunction in rats fed ethanol chronically. *World J. Gastroenterol.* **11**, 511–515 (2005).
- DeGraba, T. J. The role of inflammation after acute stroke Utility of pursuing anti-adhesion molecule therapy. *Neurology* **51**, S62–S68 (1998).
- Han, J. Y. *et al.* Chronic ethanol consumption exacerbates microcirculatory damage in rat mesentery after reperfusion. *Am. J. Physiol. -Gastr. L.* **280**, G939–948 (2001).
- Wang, M. X. *et al.* Total salvianolic acid improves ischemia-reperfusion-induced microcirculatory disturbance in rat mesentery. *World J. Gastroenterol.* **16**, 5306–5316 (2010).



15. Han, J. Y. *et al.* Potential of 3,4-dihydroxy-phenyl lactic acid for ameliorating ischemia-reperfusion-induced microvascular disturbance in rat mesentery. *Am. J. Physiol.-Gastr. L.* **296**, G36–44 (2009).
16. Han, J. Y. *et al.* Attenuating effect of Myakuryu on mesenteric microcirculatory disorders induced by ischemia and reperfusion. *Clin. Hemorheo. Micro.* **34**, 145–150 (2006).
17. Grisham, M. B., Hernandez, L. A. & Granger, D. N. Adenosine inhibits ischemia-reperfusion-induced leukocyte adherence and extravasation. *Am. J. Physiol.-Heart C.* **257**, H1334–1339 (1989).
18. Shigematsu, S., Ishida, S., Gute, D. C. & Korthuis, R. J. Bradykinin prevents posts ischemic leukocyte adhesion and emigration and attenuates microvascular barrier disruption. *Am. J. Physiol.-Gastr. L.* **277**, H161–171 (1999).
19. Panes, J. *et al.* Diabetes exacerbates inflammatory responses to ischemia-reperfusion. *Circulation* **93**, 161–167 (1996).
20. Yang, W. H., Nussbaum, C., Grewal, P. K., Marth, J. D. & Sperandio, M. Coordinated roles of ST3Gal-VI and ST3Gal-IV sialyltransferases in the synthesis of selectin ligands. *Blood* **120**, 1015–1026 (2012).
21. Wang, X. Q. *et al.* Thioredoxin interacting protein promotes endothelial cell inflammation in response to disturbed flow by increasing leukocyte adhesion and repressing Kruppel-like factor 2. *Circ. Res.* **110**, 560–568 (2012).
22. Sundd, P. *et al.* 'Slings' enable neutrophil rolling at high shear. *Nature* **488**, 399–403 (2012).
23. Sumagin, R., Kuebel, J. M. & Sarelius, I. H. Leukocyte rolling and adhesion both contribute to regulation of microvascular permeability to albumin via ligation of ICAM-1. *Am. J. Physiol.-Cell* **301**, C804–813 (2011).
24. Jang, J. E., Hod, E. A., Spitalnik, S. L. & Frenette, P. S. CXCL1 and its receptor, CXCR2, mediate murine sickle cell vaso-occlusion during hemolytic transfusion reactions. *J. Clin. Invest.* **121**, 1397–1401 (2011).
25. Gaskin, F. S. *et al.* Isoform-selective 5'-AMP-activated protein kinase-dependent preconditioning mechanisms to prevent posts ischemic leukocyte-endothelial cell adhesive interactions. *Am. J. Physiol.-Heart C.* **300**, H1352–1360 (2011).
26. Eriksson, E. E. Intravital microscopy on atherosclerosis in apolipoprotein e-deficient mice establishes microvessels as major entry pathways for leukocytes to advanced lesions. *Circulation* **124**, 2129–2138 (2011).
27. Yang, X. *et al.* Design of a real-time portable confocal scanning laser microscope. in *Photonics Asia*. (SPIE, 2012).
28. Veilleux, I., Spencer, J., Biss, D., Côté, D. & Lin, C. In vivo cell tracking with video rate multimodality laser scanning microscopy. *IEEE J. Selected Topics in Quantum Electronics* **14**, 10–18 (2008).
29. Rajadhyaksha, M., Anderson, R. & Webb, R. H. Video-rate confocal scanning laser microscope for imaging human tissues *in vivo*. *Appl. Opt.* **38**, 2105–2115 (1999).
30. Kurose, I., Wolf, R., Cerwinka, W. & Granger, D. N. Microvascular responses to ischemia/reperfusion in normotensive and hypertensive rats. *Hypertension* **34**, 212–216 (1999).
31. Thévenaz, P., Ruttimann, U. E. & Unser, M. A pyramid approach to subpixel registration based on intensity. *IEEE T. Image Process* **7**, 27–41 (1998).

Acknowledgments

We would like to thank Prof. Junlin Teng and Dr. Xuemei Hao for the help in the evaluation of the cell viability of LOSOM, and Dr. Thomas Lawson for proofreading this manuscript. This research is supported by the "973" Major State Basic Research Development Program of China (2011CB809101, 2010CB933901, 2011CB707502), the National Natural Science Foundation of China (61178076, 81072909), and PKU Med-Engineering seed grant (BMU20100114).

Author contributions

P. X. and J. H. conceived and designed the experiments. Y. D., Y. Z. and T. P. accomplished the experimental work. Y. D. and T. P. built the experimental setup and acquired data, while Y. Z. and Y. L. provided animal preparation. Y. D. and Y. L. carried out data processing and statistical analysis, while D. J. and Q. R. participated in the discussion of data analysis. Y. D., Y. Z., J. H. and P. X. drafted the manuscript together. All authors commented and approved the manuscript.

Additional information

Supplementary information accompanies this paper at <http://www.nature.com/scientificreports>

Competing financial interests: The authors declare no competing financial interests.

License: This work is licensed under a Creative Commons Attribution-NonCommercial-NoDerivs 3.0 Unported License. To view a copy of this license, visit <http://creativecommons.org/licenses/by-nc-nd/3.0/>

How to cite this article: Ding, Y.C. *et al.* Observation of mesenteric microcirculatory disturbance in rat by laser oblique scanning optical microscopy. *Sci. Rep.* **3**, 1762; DOI:10.1038/srep01762 (2013).